Determination of the Statistical Power of Longitudinally Segmented Silicon-Strip Detectors for X-ray Imaging

R. Cahn

April 10, 2001

1 General Considerations of Statistical Power

When is an observed deviation just a statistical fluctuation rather than evidence for a real effect? This most general problem confronts us in trying to identify anomalies in digital x-ray images. In ideal circumstances, the fluctuations are truly due to statistical effects and are thus easily predicted. We can also predict with confidence the effect of small bodies superimposed over a locally uniform background. Most simply, if we expect to detect n x-rays and see only $n - \nu$, the size of the deviation, measured in standard deviations, is $\nu/\sqrt{n}$, or

$$\chi_1^2 = \frac{\nu^2}{n} \tag{1}$$

Suppose that in addition to registering counts, we can measure some other variable, say, position, time, energy, etc., which we indicate by z. We can bin the events in z, so that we expect n_1 between z_0 and z_1, n_2 between z_1 and z_2, and so on. Similarly, if the extra source (or for x-rays, actually, a sink) is present, we expect instead $n_1 - \nu_1$, etc., where we suppose that $\nu_i \ll n_i$. If we determine χ^2 with the extra source present, assuming by hypothesis that it is absent, we find, on average

$$\chi_2^2 = \sum_i \frac{\nu_i^2}{n_i}, \tag{2}$$

while

$$\chi_1^2 = \frac{(\sum_i \nu_i)^2}{\sum_i n_i} \tag{3}$$

The extra information we obtained by measuring the binned variable z is $\chi^2_2 - \chi^2_1$. We can characterize this extra information by introducing two vectors,

$$\begin{aligned} a_i &= \sqrt{n_i}, \\ b_i &= \frac{\nu_i}{\sqrt{n_i}}. \end{aligned} \tag{4}$$

In terms of these

$$\begin{aligned} \chi^2_1 &= \frac{(\mathbf{a}\cdot\mathbf{b})^2}{\mathbf{a}\cdot\mathbf{a}}, \\ \chi^2_2 &= \mathbf{b}\cdot\mathbf{b}, \end{aligned} \tag{5}$$

and, continuing with the geometrical description, we define

$$\cos\theta = \frac{\mathbf{a}\cdot\mathbf{b}}{|\mathbf{a}||\mathbf{b}|}. \tag{6}$$

The parameter $\cos\theta$ characterizes how much the direction of fluctuations (the vector $\mathbf{a}$) deviates from the direction of the putative new effect (the vector $\mathbf{b}$). We can characterize the relative information available in χ^2_2 not already present in χ^2_1 as

$$\begin{aligned} \frac{\chi^2_1}{\chi^2_2} &= \cos^2\theta, \\ \chi^2_2 - \chi^1_1 &= \tan^2\theta\chi^2_1 \end{aligned} \tag{7}$$

The actual value of $\cos\theta$ depends on the binning pattern as well as the underlying distributions of n and ν as functions of z. The maximal information available is obtained by going to the continuum limit, with infinitely fine binning. This produces the minimal value of $\cos\theta$, corresponding the maximal amount of new information. It is easy to see that the replacements we need are

$$a_i \rightarrow \sqrt{\frac{dn}{dz}}$$

$$b_i \rightarrow \frac{\frac{d\nu}{dz}}{\sqrt{\frac{dn}{dz}}} \tag{8}$$

and

$$\begin{aligned} \cos^2\theta_{min} &= \frac{\left(\int dz \frac{d\nu}{dz}\right)^2}{\int dz \frac{dn}{dz} \cdot \int dz \left[(\frac{d\nu}{dz})^2 / \frac{dn}{dz}\right]} \\ &= \frac{\nu^2/n}{\int dz \left[(\frac{d\nu}{dz})^2 / \frac{dn}{dz}\right]} \end{aligned} \tag{9}$$

The latter form is particularly suggestive. It is clear that $\cos^2\theta_{min}$ is geometrical in the sense that it doesn't depend on the normalization of $n(z)$ or $\nu(z)$. If $\nu(z)$ is proportional to $n(z)$, then $\cos^2\theta = 1$.

2 Application to Digital X-ray Imaging

2.1 Using detailed energy and position information to enhance absorption measurements

Suppose we could not just count every x ray, but also measure its energy. Now let the source produce a flux $\phi(E)$. If there is an absorber with photocross-section $\sigma(E)$ and depth x so that the attenuation is $\exp(-x\sigma(E))$, the resulting flux is $\overline{\phi}(E) = \phi(E)\exp(-x\sigma(E))$. This represents dn/dz, where z here is energy. The addition of a little absorber of type b will introduce a factor $\exp(-x_b\sigma^b(E)) \approx (1 - x_b\sigma^b(E))$, so that

$$\begin{aligned} \frac{dn}{dE} &= \overline{\phi}(E) \\ \frac{d\nu}{dE} &= \overline{\phi}(E) x_b \sigma^b(E) \end{aligned} \tag{10}$$

In particular

$$\cos^2\theta_{min} = \frac{\left[\int dE\overline{\phi}(E)\sigma^b(E)\right]^2}{\int dE\overline{\phi}(E)\int dE\overline{\phi}(E)(\sigma^b(E))^2} \quad (11)$$

$$= \frac{<\sigma^b>^2}{<\sigma^{b2}>} \quad (12)$$

Here $<\ >$ indicates an average over the spectrum, $\overline{\phi}(E)$. In the case of calcium, the cross-section $\sigma^b(E)$ varies quite nearly as $1/E^3$, say $\sigma^b(E) = A_{Ca}/E^3$, over the region of interest.

In practice, the flux rises from zero starting around 20 keV and falls back to zero around 60 keV, if the source is set with 60 kVp. See Fig.(**??**). We adopt a toy model spectrum, normalized to unity:

$$\overline{\phi} = \frac{6(E_{max}-E)(E-E_{min})}{(E_{max}-E_{min})^3} \quad (13)$$

and let $r = E_{max}/E_{min}$. Then we find

$$\begin{aligned} n &= \int dE\overline{\phi}(E) = 1 \\ \nu &= \int dE\overline{\phi}(E)x_b\sigma^b(E) = \frac{6A_{Ca}E_{min}^{-3}}{(r-1)^3}x_b[\frac{1}{2}(r-\frac{1}{r})-\ln r] \\ \int dz\left[(\frac{d\nu}{dz})^2/\frac{dn}{dz}\right] &= \int dE\overline{\phi}(E)x_b^2[\sigma^b(E)]2 \\ &= \frac{6NA_{Ca}^2x_b^2E_{min}^{-6}}{(r-1)^3}[\frac{1}{12}(\frac{1}{r^3}-1)+\frac{1}{20}(r-\frac{1}{r^4})] \end{aligned} \quad (14)$$

It follows that

$$\cos^2\theta_{min} = \frac{\left[\frac{1}{2}(r-\frac{1}{r})-\ln r\right]^2}{\frac{1}{6}(r-1)^3\left[\frac{1}{12}(\frac{1}{r^3}-1)+\frac{1}{20}(r-\frac{1}{r^4})\right]} \quad (15)$$

This is shown in Fig(**??**).

Some information about the x-ray energies can be obtained by measuring where they interact in a detector. In this instance, the variable z becomes

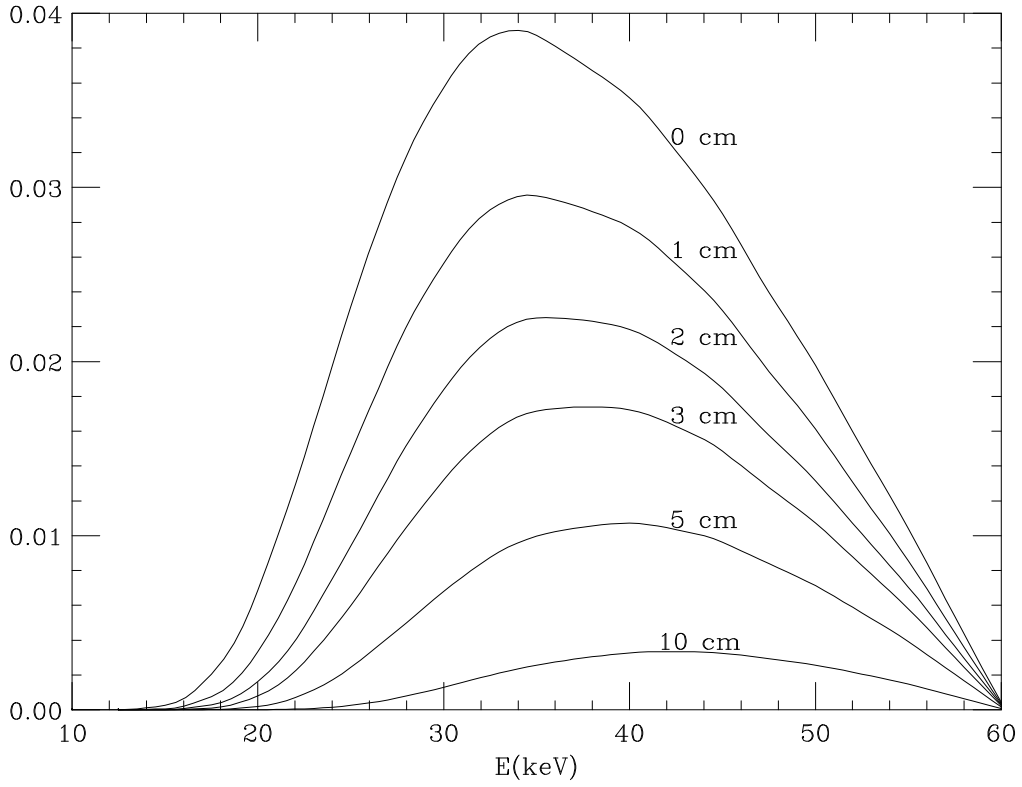

Figure 1: The spectrum from a tungsten source with 60 kVp and 2.43 mm of aluminum filter (Handbook of Mammographic X-ray Spectra, p. 41), followed through 1 cm, 2 cm, 3 cm, 5 cm, and 10 cm of "body" material, with an effective $Z = 7.4$.

the depth in the detector, x, which has units (area)$^{-1}$. The corresponding functions are

$$\begin{aligned} \frac{dn}{dx} &= \int dE \overline{\phi}(E) e^{-x\sigma(E)} \sigma(E) \\ \frac{d\nu}{dx} &= \int dE \overline{\phi}(E) e^{-x\sigma(E)} \sigma(E) x_b \sigma^b(E) \end{aligned} \tag{16}$$

Here $\sigma(E)$ is the photo-cross-section in the silicon detector, while $\sigma^b(E)$ is again the cross-section in calcium. We see immediately that

$$\begin{aligned}\int_0^\infty dx\frac{dn}{dx} &= \int dE\overline{\phi}(E) = n = 1 \\ \int_0^\infty dx\frac{d\nu}{dx} &= \int dE\overline{\phi}(E) = \nu = x_b\sigma^b(E) = x_b < \sigma^b > \end{aligned} \tag{17}$$

There remains to calculate

$$\int_0^\infty dx \left\{ \frac{\left[\int dE\overline{\phi}(E)e^{-x\sigma(E)}\sigma(E)x_b\sigma^b(E)\right]^2}{\int dE\overline{\phi}(E)e^{-x\sigma(E)}\sigma(E)} \right\} \tag{18}$$

We continue with our toy model for $\overline{\phi}$, and take $\sigma(E)$ also to vary as $1/E^3$, $\sigma(E) = A(Si)/E^3$. The calculations of n and ν are, of course, unchanged. In addition, we have

$$\int dx \left[(\frac{d\nu}{dx})^2/\frac{dn}{dx}\right] = \frac{6[\sigma^b(E_{min})]^2x_b^2}{E_{min}^6(r-1)^3}\int_0^\infty dt \left\{ \frac{\left(\int_1^r ds(r-s)(s-1)e^{-t/s^3}s^{-6}\right)^2}{\int_1^r ds(r-s)(s-1)e^{-t/s^3}s^{-3}} \right\} \tag{19}$$

The results are shown in Fig. (**??**).

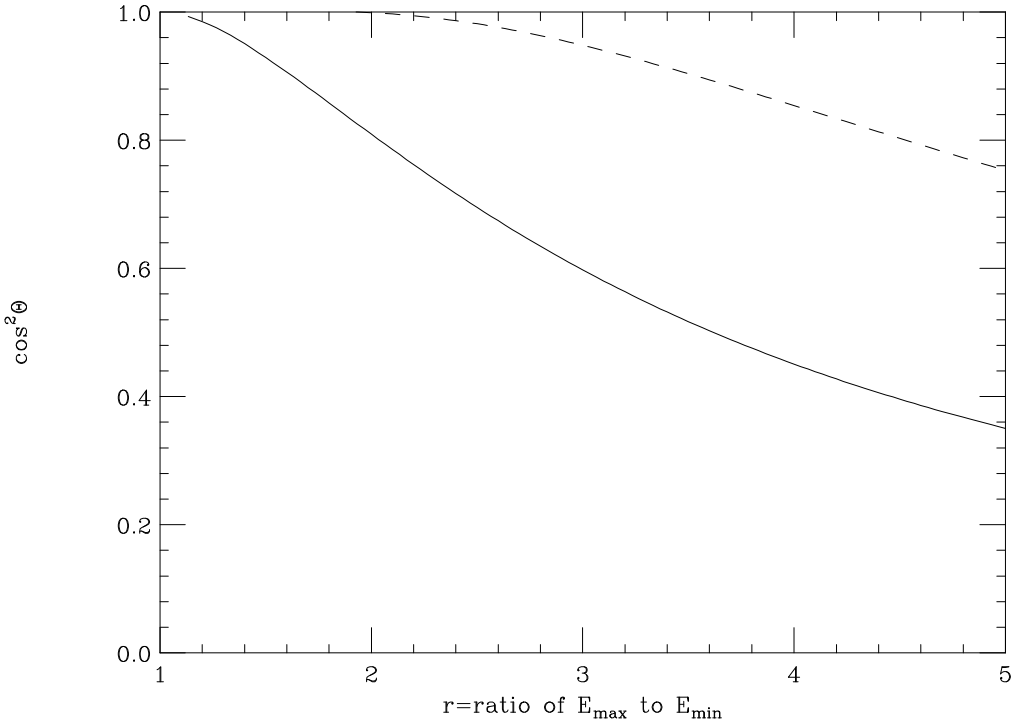

Figure 2: The ratio $\chi_1^2/\chi_2^2 = \cos^2\theta$ as a function of the ratio $r = E_{max}/E_{min}$, where E_{max} and E_{min} are the upper and lower ends of the x-ray spectrum, Eq. (??). The full line corresponds to measurement of the actual energy of each x-ray, while the dashed line corresponds to measuring the position of the x-ray's interaction in the detector. In both cases, it is assumed that the measurements are perfect. The lower the value of $\cos^2\theta$, the more information is being provided by the energy or position measurement.

2.2 Distinguishing calcium from ordinary tissue using energy and position measurements

Suppose we know we have a significant deviation from background. We wish to determine whether it is due to substance a or substance b. In our range of interest, 20 - 60 keV and $6 \leq Z \leq 20$, the photo-cross-section in barns can be approximated by

$$\sigma = 24.15 Z^{4.20} E^{-3} + 0.56 Z \tag{20}$$

where E is measured in keV. See Fig. (**??**). Suppose, now, that the total number of events in the deviation is ΔN. This could be due to x_a of substance a or x_b of substance b. The units for x_a and x_b are atoms/barn. Their values are determined by

$$\begin{aligned} \Delta N &= N x_a \int dE \overline{\phi}(E) \sigma^a(E) = N x_a < \sigma^a > \\ \Delta N &= N x_b \int dE \overline{\phi}(E) \sigma^b(E) = N x_b < \sigma^b > \end{aligned} \tag{21}$$

Can we distinguish the two alternatives on the basis of detailed measurements of the energy or position distribution of the events?

Let us start with the hypothesis that the cause is substance a. Now if, in fact, the cause is substance b, we should see a deviation from our hypothesis that can be quantified by

$$\chi^2_E = N \int dE \frac{(\frac{d\nu_a}{dE} - \frac{d\nu_b}{dE})^2}{\frac{dn}{dE}} \tag{22}$$

where

$$\begin{aligned} \frac{d\nu_a}{dE} &= x_a \overline{\phi}(E) \sigma^a(E) \\ \frac{d\nu_b}{dE} &= x_b \overline{\phi}(E) \sigma^b(E) \\ \frac{dn}{dE} &= \overline{\phi}(E) \end{aligned} \tag{23}$$

Altogether, we can write

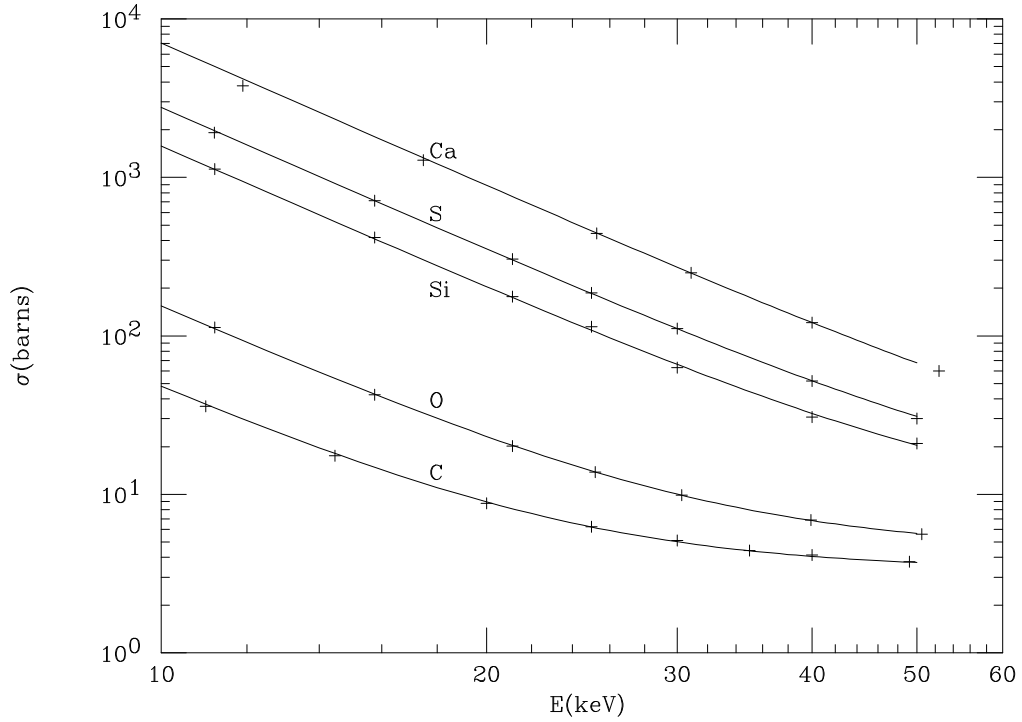

Figure 3: The photo-cross-section for calcium, sulfur, silicon, oxygen, and carbon for energies between 10 and 50 keV. The curves are a fit to the theoretical points shown as crosses. The fit is given by $\sigma = 24.15Z^{4.20}E^{-3} + 0.56Z$, where σ is in barns and E is in keV.

$$\begin{aligned}
\chi^2_E &= N x_a^2 \int dE \overline{\phi}(E)(\sigma^a(E) - \frac{x_b}{x_a}\sigma^b(E))^2 \\
&= N x_a^2 \left\langle (\sigma^a - \frac{x_b}{x_a}\sigma^b)^2 \right\rangle \\
&= \frac{(\Delta N)^2}{N < \sigma^a >^2} \left\langle (\sigma^a - \frac{x_b}{x_a}\sigma^b)^2 \right\rangle \\
&= \chi^2_1 \frac{\left\langle (\sigma^a - \frac{x_b}{x_a}\sigma^b)^2 \right\rangle}{< \sigma^a >^2}
\end{aligned} \tag{24}$$

See Fig. **??**.

For a specific example, suppose $E_{min} = 20$ keV and $E_{max} = 60$ keV. We find for a=oxygen and b=calcium

$$\begin{aligned} < \sigma^a > &= \int dE\overline{\phi}(E)\sigma^a(E) = 7.8 \text{ barns} \\ < \sigma^b > &= \int dE\overline{\phi}(E)\sigma^b(E) = 166. \text{ barns} \end{aligned} \tag{25}$$

and

$$x_b/x_a = 0.047 \tag{26}$$

Numerically, we find

$$\chi^2_E = 0.17\chi^2_1 = 0.17\frac{(\Delta N)^2}{N} \tag{27}$$

One millimeter of oxygen at a density of 1 g/cm^3 gives 3.75×10^{-3} atoms/barn. Multiplying by 7.8 barns, the average cross section, we get an interaction probability of 2.9×10^{-2} per millimeter. If $N = 10^5$, then $\chi^2_1 = (0.029)^2 \times 10^5 = 84$ and the energy measurement separation of a and b has $\chi^2 = 14$.

Next consider what can be achieved if we measure only position. We suppose that we can measure precisely the distribution of "excess" events as a function of x. We have

$$\begin{aligned} \chi^2_x &= N\int dx \frac{(\frac{d\nu_a}{dx} - \frac{d\nu_b}{dx})^2}{\frac{dn}{dx}} \\ &= Nx_a^2 \int dx \frac{[\int dE\overline{\phi}e^{-x\sigma}\sigma(\sigma^a - \frac{x_b}{x_a}\sigma^b)]^2}{\int dE\overline{\phi}e^{-x\sigma}\sigma} \\ &= \chi^2_1 \int dx \frac{[\int dE\overline{\phi}e^{-x\sigma}\sigma(\sigma^a - \frac{x_b}{x_a}\sigma^b)]^2}{< \sigma^a >^2 \int dE\overline{\phi}e^{-x\sigma}\sigma} \end{aligned} \tag{28}$$

In Fig. (**??**) we show $d\nu/dx$. Because $\int dE\overline{\phi}(E)[\sigma^a - (x_a/x_b)\sigma^b] = 0$, the integrand must vanish somewhere. In Fig. (**??**) we see that this occurs at $x \approx 0.02$ barn^{-1}, i.e. 4 mm of silicon.

Numerically, we find

$$\chi^2_x = 0.022\chi^2_1 \tag{29}$$

In the case considered above, with $N = 10^5$ and $\chi^2_1 = 84$, we have $\chi^2_x = 1.84$, which may not seem impressive, but this is for the equivalent of 47μm of calcium! Note that χ^2_x scales as x_a^2 or x_b^2.

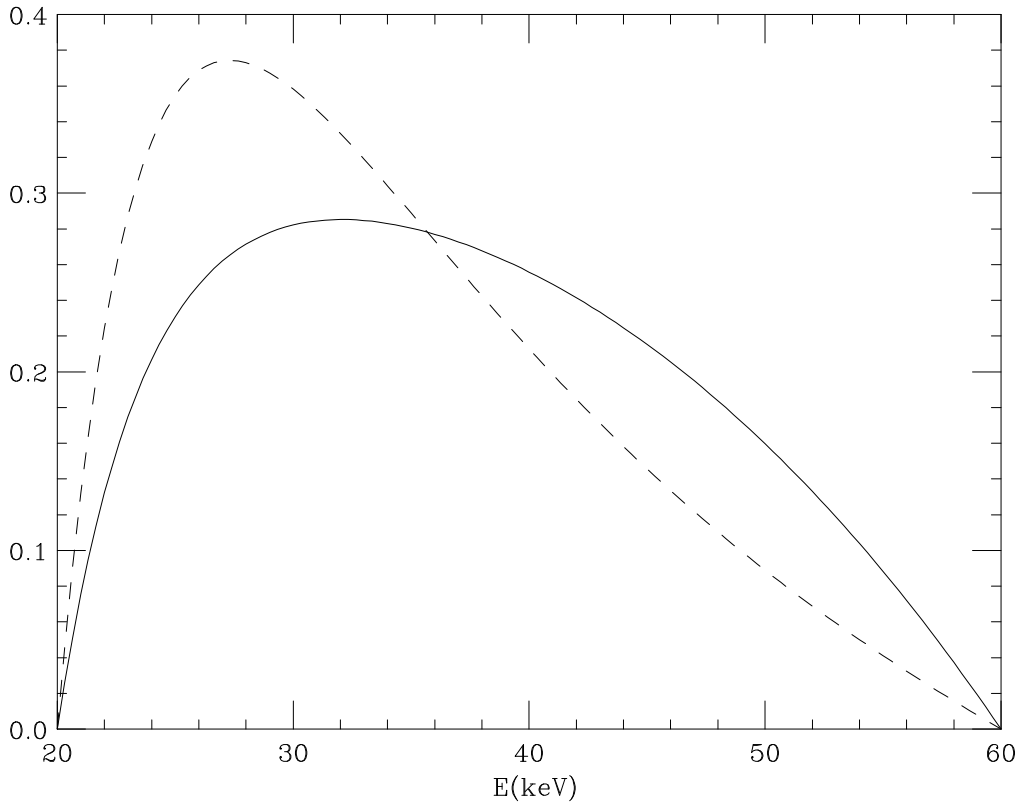

Figure 4: The differential energy distribution of x rays from oxygen (solid) and calcium (dashed). The calcium cross section is scaled down by the ratio of the mean cross sections of oxygen and calcium, so that it represents the same total absorption, a reduction by a factor 0.047. The quantity plotted for oxygen is $(1/x_a)d\nu_a/dE$ in barns/keV, with the analogous scaled quantity plotted for calcium. The incident spectrum is as given in the text, with a range from 20 keV to 60 keV.

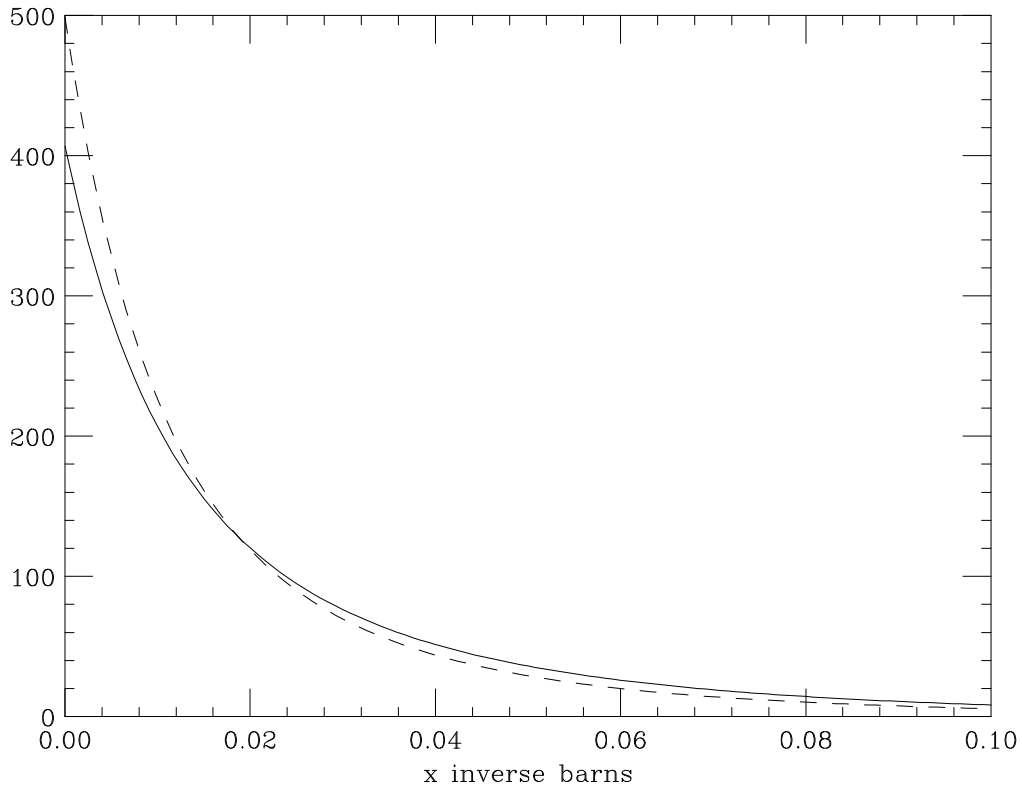

Figure 5: The differential distribution in position for x rays interacting in a silicon detector. The deficits due to a deposit of oxygen (solid) or a deposit of calcium (dashed) are shown. The calcium cross section is scaled down by the ratio of the mean cross sections of oxygen and calcium, so that it represents the same total absorption, a reduction by a factor 0.047. The quantity plotted for oxygen is $(1/x_a)d\nu_a/dx$, in barns^2. The incident spectrum is as given in the text, with a range from 20 keV to 60 keV. The density of silicon is 0.049 /barns/cm^{-1}.

3 Dual-Energy Scheme

It might be possible to generate an x-ray beam whose spectrum is concentrated at two energies. We consider here the discriminating capability of such a beam in the approximation that the spectrum consists of two delta functions in energy, the energies being E_α and E_β. The fraction of the flux at E_α is α and that at E_β is $\beta = 1 - \alpha$. Using the formulas of the previous sections and the flux

$$\overline{\phi}(E) = \alpha\delta(E - E_\alpha) + \beta\delta(E - E_\beta) \tag{30}$$

we find the results shown in Fig. (**??**).

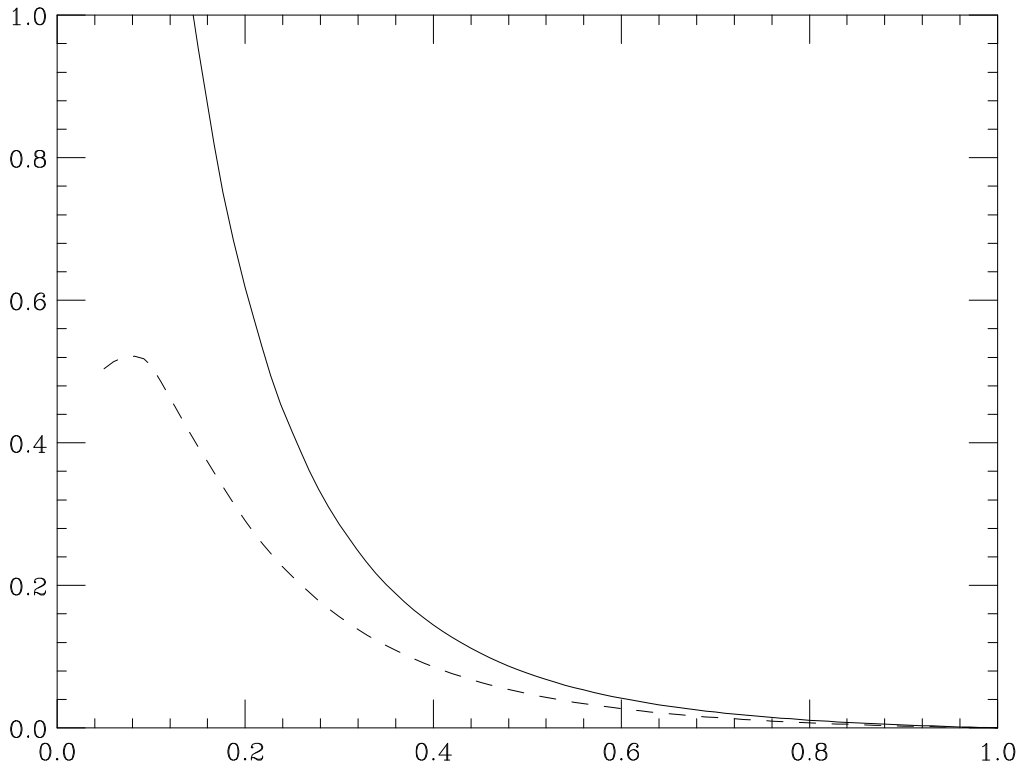

Figure 6: The ratio of χ^2_E to χ^2_1 (solid) and ratio of χ^2_x to χ^2_1 (dashed) as a functions of α, the fraction of the spectrum at 20 keV (the remainder being at 60 keV).

Consider a practical example with 20% of the spectrum at 20 keV and 80% at 60 keV. Suppose we have 50 μm of calcium and we want to distinguish it from an amount of ordinary (compressed?) tissue with the same total absorption. Suppose the detector has two segments, the first 0.4 cm long, the second effectively infinitely long. The 0.4 cm of silicon amounts to 0.0196 b^{-1} as a number density.

The relevant cross-sections are shown in Table **??**.

	20 keV (b)	60 keV (b)
σ(Si)	204	15
σ(Ca)	890	44
σ(O)	23	5.2

Table 1: Cross-sections in barns for x rays on silicon, calcium, and oxygen, the last being chosen as representative of body tissue.

Of the low energy component, only $\exp(-0.0196 \times 204) = .0198$ makes it to the second segment, while of the high energy component, $\exp(-0.0196 \times 15) = 0.745$ does. In this way we find that 0.4 of the total spectrum stops in the first segment and 0.6 in the second.

The 50 μm of calcium amounts to a number density of 1.14×10^{-4} b^{-1}. This depletes $1.14 \times 10^{-4} \times 890 = 0.101$ of the low energy component and $1.14 \times 10^{-4} \times 44 = 0.0050$ of the high energy component. Altogether, 0.024 of the beam is attenuated. An equivalent depth of "oxygen" would be $2.77 \times 10^{-3}\mathrm{b}^{-1}$.

A straightforward calculation yields Table **??**.

To be even more concrete, consider $N = 10^5$ x rays. The depletion amounts to 0.024×10^6, a 24 sigma effect. In terms of the quantities discussed above, we have

$$\chi_1^2 = \frac{(0.024 \times 10^6)^2}{10^6} = 576 \tag{31}$$

The χ^2 for the hypothesis that the depletion is due to "oxygen" when it is really due to calcium is expected to be

$$\chi_x^2 = \frac{[(1.54 - 2.09) \times 10^4]^2}{0.4 \times 10^6} + \frac{[0.88 - 0.34) \times 10^4]^2}{0.6 \times 10^6} = 113 \tag{32}$$

	segment 1	segment 2
total	0.4	0.6
depleted by calcium	0.0209	0.0034
depleted by "oxygen"	0.0154	0.0088

Table 2: Fraction of the beam absorbed in the two segments, the first of which is 0.4 cm deep. The beam is 20% 20 keV and 80% 60 keV. The amount of "oxygen" is adjusted to give the same total depletion as 50 μm of calcium.

The ratio $\chi^2_x/\chi^2_1 = 0.20$ is slightly less than predicted by our model with an infinite number of segments, rather than two.